Acoustic Field-Assisted Two-Photon Polymerization Process

Ketki M. Lichade
Department of Mechanical and Industrial Engineering,
University of Illinois at Chicago,
Chicago, IL 60607
e-mail: klicha2@uic.edu

Yayue Pan[1]
Department of Mechanical and Industrial Engineering,
University of Illinois at Chicago,
Chicago, IL 60607
e-mail: yayuepan@uic.edu

This study successfully integrates acoustic patterning with the Two-Photon Polymerization (TPP) process for printing nanoparticle–polymer composite microstructures with spatially varied nanoparticle compositions. Currently, the TPP process is gaining increasing attention within the engineering community for the direct manufacturing of complex three-dimensional (3D) microstructures. Yet the full potential of TPP manufactured microstructures is limited by the materials used. This study aims to create and demonstrate a novel acoustic field-assisted TPP (A-TPP) process, which can instantaneously pattern and assemble nanoparticles in a liquid droplet, and fabricate anisotropic nanoparticle–polymer composites with spatially controlled particle–polymer material compositions. It was found that the biggest challenge in integrating acoustic particle patterning with the TPP process is that nanoparticles move upon laser irradiation due to the photothermal effect, and hence, the acoustic assembly is distorted during the photopolymerization process. To cure acoustic assembly of nanoparticles in the resin through TPP with the desired nanoparticle patterns, the laser power needs to be carefully tuned so that it is adequate for curing while low enough to prevent the photothermal effect. To address this challenge, this study investigated the threshold laser power for polymerization of TPP resin (P_{thr}) and photothermal instability of the nanoparticle (P_{thp}). Patterned nanoparticle–polymer composite microstructures were fabricated using the novel A-TPP process. Experimental results validated the feasibility of the developed acoustic field-assisted TPP process on printing anisotropic composites with spatially controlled material compositions. [DOI: 10.1115/1.4050759]

Keywords: two-photon polymerization, nanoparticle–polymer composite, acoustic field, particle assembly, additive manufacturing

1 Introduction

Micro-manufacturing techniques have been drastically investigated over the past decades for applications such as microfluidic devices [1], biochips [2], photonic crystals [3], and micro-electromechanical systems (MEMS) [4]. Advances in many micro-manufacturing techniques have been reported, including soft lithography [5], electrochemical fabrication [6], chemical deposition [7], immersing [8], laser microfabrication [9], imprinting [10], and two-photon polymerization (TPP) [11]. Among these techniques, TPP has been considered as a promising technique for direct manufacturing of complex three-dimensional (3D) micro/nanostructures [12], wherein a photosensitive liquid resin gets polymerized at the center of the tightly focused beam and the three-dimensional (3D) digital model is built in a voxel by voxel manner [13]. Considering these advantages, many research studies have investigated TPP to create 3D complicated nano/microstructures [14] for varied applications, including photonic quasicrystals [15], metamaterials [16], functional micro/nano-mechanical devices [17], cell culturing 3D scaffolds for tissue engineering [18,19], and optical data storage devices [20].

The typical materials used in the TPP process are negative resists, such as IP-S or IP-L [21], and positive resists, such as AZ [22]. Like most photopolymerization-based 3D printing techniques, a significant challenge of polymer materials used in TPP technique is the relatively poor mechanical properties of the printed microstructures compared to their counterparts fabricated by other techniques such as molding or filament extrusion 3D printing process and hence are not suitable for many practical applications. To solve the problem of limited structural/mechanical performance of polymers used in the TPP process, efforts have been put forth to add different types of functional fillers [23,24], creating homogeneous composites. Functional fillers investigated in the TPP process include carbon-based materials [25], photoisomerizable dyes [26], semiconductor nanoparticles [27], metallic nanoparticles [28], and magnetic nanoparticles [29]. For instance, Liu et al. found that the loading of multi walled carbon nanotubes (MWNTs) can significantly enhance Young's modulus and hardness of the microstructures fabricated by the TPP process [30]. Moreover, Ovsianikov et al. demonstrated the advantage of zirconium fillers for minimizing shrinkage [31].

Recent studies have proved that, along with the loading fraction, particle alignment plays a vital role in designing structures with tunable properties [32,33]. A number of techniques have been developed to align functional fillers in the polymer matrix [34] using external force, including magnetic [35–38], electric [39–42], and acoustic fields [43–47]. Martin et al. [36] and Lu et al. [37] integrated the magnetic field in a stereolithography system to achieve varied orientations and loading fractions of particles. Many other researchers, such as Yang et al. [40], fabricated bioinspired composite structures by implementing a rotating electric field to align carbon nanotubes radially in a projection stereolithography system. It was observed that the particle alignment significantly influences Young's modulus and many other physical properties such as electrical conductivity. However, a major limitation of the magnetic field and the electric field-assisted methods is that the particles have to be naturally responsive to the applied external field.

Compared to the magnetic or electric field, the acoustic field-assisted additive manufacturing process has the advantage of no imposed material shape/size constraints and no field-responsive requirements. In addition, patterning using an acoustic field is gentle enough for the manipulation of fragile particles or living cells, and any combination of fillers and host materials is suitable as long as there is an acoustic contrast [48,49]. Implementation of the acoustic field for particle aligning during fabrication has been reported in a few studies. For example, acoustic assembly of electrically conductive particles was demonstrated by Yunus et al. [43]. Collino et al. demonstrated the use of acoustic focusing to successfully deposit composite filaments consisting of fibers and microspheres using a single nozzle [44]. Moreover, Lu et al. successfully printed composites that contained acoustically assembled tungsten, aluminum, titanium, and copper particles with desired patterns [46].

Despite the extensive research on the integration of acoustic patterning with additive manufacturing (AM) processes, most studies focused on stereolithography (SL), direct ink writing (DIW), and fused deposition modeling (FDM)-based AM processes [50]. To the author's best knowledge, no study has been reported about integrating an acoustic field into the TPP process to print microstructures with aligned nano-fillers. A major challenge in integrating external field-assisted (e.g., acoustic field-assisted) particle patterning into the TPP process is that nanoparticles move upon laser irradiation due to the photothermal effect, and hence, the acoustic assembly is distorted during the photopolymerization process

[1]Corresponding author.
Manuscript received July 21, 2020; final manuscript received March 28, 2021; published online April 30, 2021. Assoc. Editor: Gary J. Cheng.

[51]. This makes it very difficult or even impossible to cure nanoparticle–polymer composite microstructures with desired nanoparticle patterns. Several strategies have been employed in the TPP industry to overcome the photothermal effect. A common method is to introduce solvent molecules, including water [52], ruthenium-based dye [53], and initiators [54] into the original resin mixture. For instance, Liu et al. created 3D gold–polymer microstructures by adding ruthenium-based dye [53]. Hu et al. used 7-diethylamino-3-thenoylcoumarin (DETC) as a photoinitiator to successfully fabricate complex 3D Au-containing nanocomposite structures [54]. This method allows for some flexibility in tailoring the photothermal effect; however, the loading fraction and the choice of nanoparticles were both very limited.

An alternative strategy was proposed by Masui et al., which involves polymerizing the material using a laser power much lower than the threshold for initiating the particle photothermal instability [51]. However, the typical polymerization threshold of the laser power for ordinary TPP resin is an order of magnitude larger than the threshold of the photothermal instability of particles. Pentaerythritol tetrakis (thiol) has been reported effective in lowering the threshold laser power for the polymerization of acrylate resin used in the TPP process [55]. Reported work in these and other references, e.g., Refs. [56–58], demonstrated that thiol molecules were able to improve the conversation rate of acrylate resin, suggesting the addition of multifunctional thiol molecules is a promising method to reduce the threshold power for the polymerization of resin (P_{thr}). A common challenge with this method is that too much thiol reduces the minimum feature size, leading to various manufacturing defects in the fabricated structures. So, there is an urgent need for developing a general strategy to balance the threshold powers for polymerization of acrylate resin using thiol molecules and (P_{thr}) and photothermal instability of the nanoparticle (P_{thp}).

Here, we present an acoustic-field-assisted two-photon polymerization (A-TPP) process for fabricating heterogeneous composite microstructures with desired nanoparticle patterns. To develop a strategy for achieving a balance between the two threshold powers P_{thr} and P_{thp}, the threshold laser powers for the polymerization of IP-L 780 photoresist (P_{thr}) with thiol concentration ranging from 0% to 30% by weight were investigated. In addition, threshold laser powers for photothermal instability of various nanoparticles (P_{thp}) were experimentally identified by observing the movement of nanoparticle during TPP printing. The analytical model was developed as a guide to select minimum thiol concentration and safe operating laser power during the A-TPP process to fabricate defect-free high-quality microstructures. With the determined thiol concentration and laser power, the acoustic field generation system was then integrated into the TPP process to pattern nanoparticles in the resin droplet. To demonstrate the feasibility of this method, patterned nanoparticle–polymer composite microstructures were fabricated by repeating the acoustic assembling and two-photon polymerizing procedure. Test results illustrated the feasibility of the novel A-TPP process for the successful production of heterogeneous composite microstructures with desired particle patterns, locally controlled particle concentrations, and orientations. The rest of the article is organized as follows: Sec. 2 describes the proposed A-TPP process. Section 3 develops an experimental model to predict the appropriate laser power and presents a test case to validate the feasibility of the proposed method. Lastly, Sec. 4 summarizes this study and its findings.

2 Method and Experimental Setup

2.1 Overview of the A-TPP Process and Setup. In this study, synthetic black iron oxide spherical nanoparticles (Alpha Chemical, Stoughton, MA) were used as functional fillers. The average diameter of spherical iron oxide particles was about 20 nm. IP-L 780 photoresist (Nanoscribe GmbH, Eggenstein-Leopoldshafen, Germany) was used as the base material. Its bright yellow color makes it easy to observe the iron oxide particles in a microscope during and after TPP printing. In addition to base and filler materials, 1% of Irgacure photoinitiator (Sigma-Aldrich, St. Louis, MO) and varied wt.% of thiol molecules (Sigma-Aldrich, St. Louis, MO) were added to prepare the composite mixture samples. The procedure for the material preparation is illustrated in Fig. 1(*a*). First, iron oxide spherical nanoparticles were added into photoresist containing 1% by weight of the photoinitiator. The solution was vigorously stirred for 2 min and then left for 48 h at room temperature. After forming a homogeneous solution, thiol was added with weight fractions ranging from 0 to 30 wt.% and stirred for 2 min.

A circular-shaped piezoelectric plate (R, 7.5 mm; h, 0.7 mm) was incorporated onto the substrate in the TPP printer to align nanoparticles and create microstructures. According to Wadsworth et al., smaller pattern thickness can be obtained at higher frequencies [59]. Therefore, the piezoelectric plate with resonant frequency as high as 3 MHz was selected (Steiner & Martins, Inc., Davenport, FL). This plate was placed on the top of the Kapton tape, as shown in Fig. 1(*b*). The signal was generated by a function generator (RIGOL Technologies Inc., Beijing, China) and amplified (TEGAM Inc., Geneva, OH) to actuate the piezoelectric plate. The actuated piezoelectric plate created acoustic waves in the composite resist mixture, which drove nanoparticles to the wave nodes/antinodes and hence assembled particles to the desired pattern.

A commercial two-photon polymerization (TPP) (Nanoscribe GmbH, Eggenstein-Leopoldshafen, Germany) setup was retrofitted

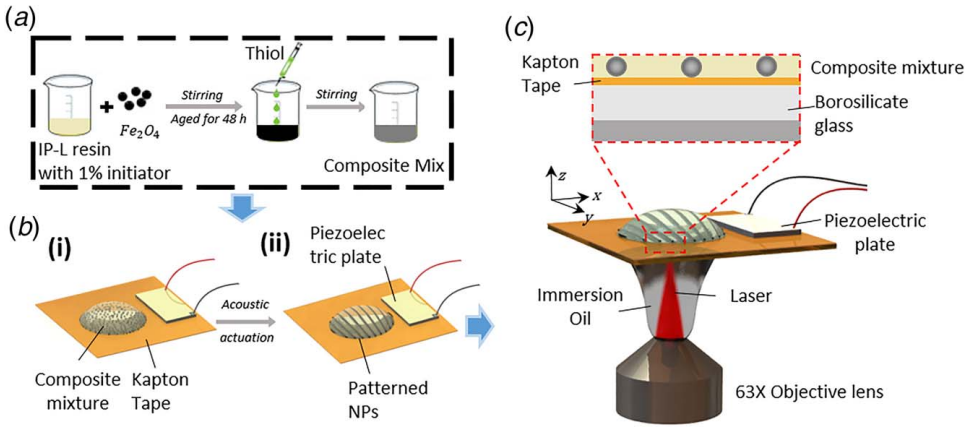

Fig. 1 Procedure for the fabrication of nanoparticle–polymer composite microstructures using the proposed A-TPP process: (*a*) procedure for sample preparation; (*b*) acoustic patterning of nanoparticles in a liquid composite drop; and (*c*) schematics of the experimental setup

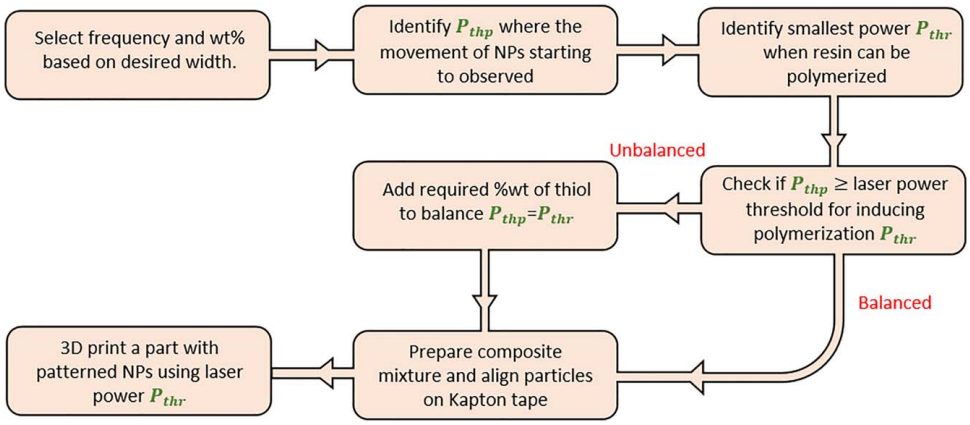

Fig. 2 Flowchart for identifying the minimum thiol concentration and safe operating laser power during A-TPP process

to demonstrate the feasibility and effectiveness of incorporating acoustic patterning into the TPP process. The system allows users to tune the laser power in percent from 0 to 100. A laser power of about 30% is usually used for curing the pure IP-L 780 photoresist in standard piezo scan mode. A 100% ratio is a laser power of 50 mW. Among various substrates, Kapton tape has been proven to be highly responsive to the acoustic field for the manipulation of particles [60] and nanostructures [61]. Therefore, in the retrofitted TPP system, a piece of acoustic-responsive thin Kapton tape was placed on the borosilicate glass substrate to accommodate the short focal length of the objective lens and meanwhile facilitate the acoustic patterning process. The retrofitted setup consists of a laser system, a scanning system, and an acoustic system, as shown in Fig. 1(*c*). A femtosecond pulsed laser emitting at 780 nm, with a pulse width of 100 fs and a repetition rate of 80 MHz, was used as the light source to polymerize the acoustically patterned composite mixture. The piezoelectric stage was utilized for scanning in the *x*, *y*, and *z* directions. The Kapton tape with patterned nanoparticle–composite mixture and the piezoelectric plate was then transferred on the top of the borosilicate glass substrate. In addition, a small amount of immersion oil was dropped on the bottom side of the substrate. The modified substrate was then mounted on a linear stage via a substrate holder.

2.2 Fabrication of Anisotropic Composite Structures Using the A-TPP Process. Figure 2 shows the flowchart for identifying the minimum thiol concentration and safe operating laser power to fabricate defect-free nanoparticle–polymer composite microstructures using the proposed A-TPP process. The process starts with an initialization step defining the particle pattern thickness, wt.% of nanoparticles, and actuation frequency. For a given wt.% of iron oxide, P_{thp} was then identified by capturing the movement of nanoparticles using a high-speed camera. In addition, the threshold laser power for the polymerization of TPP resin (P_{thr}) was characterized. If P_{thr} is greater than P_{thp}, an appropriate amount of thiol molecules, based on the developed statistical model, must be added into the composite mixture to lower polymerization threshold down to P_{thp}. Once the power thresholds were balanced, the nanoparticles were acoustically patterned on the Kapton tape and nanoparticle–polymer composite microstructures were cured on the modified substrate by laser

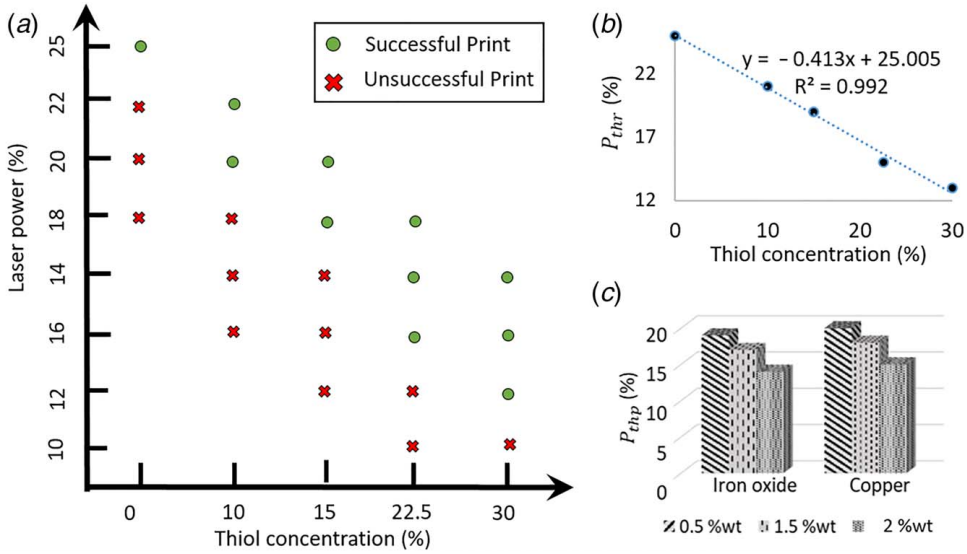

Fig. 3 Study of threshold laser power: (*a*) printing results with changing laser power and wt.% of thiol; (*b*) relation between the wt.% of thiol and threshold laser power for polymerization (P_{thr}) of IP-L 780 photoresist; and (c) threshold laser power for inducing the photothermal instability (P_{thp}) for resin mixtures with iron oxide and copper nanoparticles at different loading fractions

irradiation using the A-TPP process. Finally, the samples were developed using SU-8 (MicroChem Corp., Newton, MA) for 9 min, followed by cleaning in an isopropyl alcohol (IPA) (Sigma-Aldrich, St. Louis, MO) for 2 min and air drying.

3 Results and Discussion

3.1 Analytical Modeling of Threshold Intensities. This section aims to develop a strategy for identifying the safe laser power and appropriate concentration of multifunctional thiol molecules to induce the polymerization at a power lower than or equal to the photothermal instability threshold of nanoparticles. For this purpose, we performed two experiments. The first experiment investigates the effect of thiol concentration on the P_{thr}, and the second focuses on identifying the P_{thp} values by observing the nanoparticle movement upon laser irradiation. In addition to the iron oxide nanoparticles studied in the test cases, copper nanoparticle was also tested in the second experiment.

In the first experiment, five mixtures were prepared by mixing IP-L 780 photoresist with thiol molecules with concentrations of 0%, 10%, 15%, 22.5%, and 30% by weight. A set of square samples with dimensions of 100 μm wide by 100 μm long by 1 μm thick were fabricated at a fixed writing speed of 20 mm/s, a 0.4 μm slicing layer thickness, and a 0.3 μm hatching distance, but with the laser power level progressively decreasing by 2% starting from the 25% level. If the printed part has defects such as incomplete geometry or behaving like a gel, the printing result was marked as an unsuccessful printing. The experimental results are plotted in Fig. 3(*a*). The lowest laser power that enabled successful printing was identified as the threshold P_{thr} for the related thiol concentration. As shown in Fig. 3(*a*), a remarkable reduction in P_{thr} was observed as the concentration of thiol molecules in the resin mixture increased. For example, by adding thiol concertation of 22.5%, the lowest printable laser power was reduced from 25% (without thiol) to 14%. Moreover, the presence of 30% by weight of the thiol molecule in the IP-L 780 photoresist reduces P_{thr} from

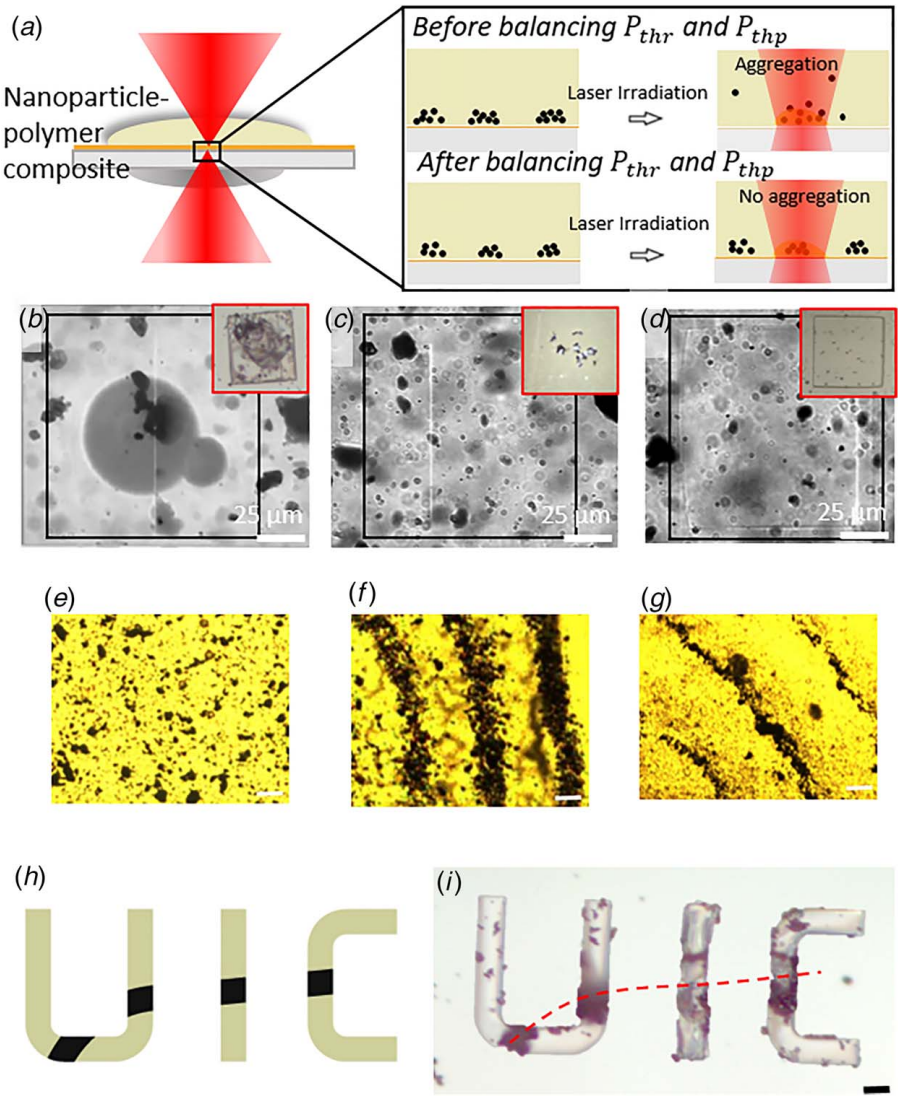

Fig. 4 Fabrication of nanoparticle–polymer composite microstructures using the novel A-TPP process: (*a*) illustration of mechanisms for the formation of microstructures without and with the balancing of the laser power thresholds; composite printing using the laser power of (*b*) 25% = P_{thr} (>P_{thp}), (c) 19% = P_{thp} (<P_{thr}), (*d*) 19% = P_{thr} = P_{thp} (10% thiol); (*e*) microscopic image of prepared sample before applying the acoustic field; (*f*) curve patterned 0.5 wt.% iron oxide sample at frequency 44 kHz (scale bar: 50 μm); (*g*) curve patterned 0.5 wt.% iron oxide sample at frequency 2.2 MHz; (*h*) CAD model of letters "UIC"; and (*i*) an optical image of letters "UIC" printed using the proposed method with locally distributed iron oxide nanoparticles along the center (scale bar: 20 μm)

25% to 12%. Figure 3(*b*) shows the relationship between the threshold laser power for polymerization P_{thr} and the thiol wt.% for 1% initiator concentration in the mixture. Let x be the wt.% of thiol molecules, based on the experimental results, the relationship can be modeled as follows:

$$P_{thr} = -0.413\,x + 25.005 \tag{1}$$

In the second experiment, three mixtures were prepared by mixing IP-L 780 photoresist with nanoparticles with concentrations of 0.5%, 1.5%, and 2% by weight. To investigate the threshold power for photothermal instability of nanoparticles (P_{thp}), the laser power was gradually increased and the movement of the resulting nanoparticles was monitored using a high-speed camera (AxioCam MRM). The value of P_{thp} at which the movement of nanoparticles due to the photothermal effect starts to be observed was recorded and plotted in Fig. 3(*c*). The test was repeated for iron oxide and copper nanoparticles with concentrations ranging from 0.5% to 2% in weight. The observed results and the experimentally fitted model Eq. (1) were used to identify the minimum thiol concentration and the safe laser power for printing nanoparticle–polymer composite microstructures using the A-TPP process, as discussed in Sec. 3.2.

3.2 Test Case. Our hypothetical mechanisms for the formation of nanoparticle–polymer composite microstructures without and with balancing threshold intensities are illustrated in Fig. 4(*a*). Under the unbalanced condition, when the laser power equal to P_{thr} ($>P_{thp}$) is applied, a sudden temperature increase is found around the irradiated nanoparticles, resulting in a quick movement of nanoparticles and then bubbling of resin, which is known as the photothermal effect. As a result, the nanoparticle pattern in the resin gets distorted, and the desired nanocomposite structure cannot be achieved. On the other hand, if the laser power equaling to the threshold for photothermal instability P_{thp} ($<P_{thr}$) is applied, the photothermal effect would be eliminated, but the polymerization of liquid resin cannot occur as a result of the insufficient laser power. On the contrary, under the balanced laser irradiation where the applied laser power is P_{thp} ($= P_{thr}$), nanoparticle assembly maintains the pattern and photoresin can get fully cured into the desired shape.

To test the above-mentioned hypotheses and validate the effectiveness of the proposed acoustic field-assisted TPP method, experiments were conducted to test the aforementioned three cases. We prepared the composite mixture using IP-L 780 photoresist with a 1% photoinitiator and 0.5 wt.% iron oxide nanoparticles. For case 1, the printing power selected was 25%, which is equal to P_{thr} but greater than P_{thp}. As shown in Fig. 4(*b*), the prepared composite was curable, but at such high power, obvious photothermal effects of nanoparticles were observed along with part defects caused by bubbles. Moreover, aggregation of nanoparticles was observed during printing. For case 2, the same composite mixture was printed with 19% laser power, which is equal to P_{thp} but smaller than P_{thr}. As shown in Fig. 4(*c*), no photothermal instability issues such as bubbling or aggregation were observed, but such a low power failed to induce the polymerization reaction. To lower P_{thr} down to 19%, according to Eq. (1), we added approximately 10% (weight ratio) of thiol molecules into the particle–polymer composite. In case 3, this particle–polymer–thiol composite was tested with a laser power of 19%, which is equal to P_{thp} and P_{thr}. We observed that the aggregation and bubbling of nanoparticles (NP) did not occur, and the final printed geometry had the desired shape, as shown in Fig. 4(*d*). The experimental observations validated our hypotheses, suggesting that balancing threshold laser powers is critical for printing a composite mixture, which can be done by adding the required amount of thiol molecules to lower down the polymerization laser power threshold P_{thr} to the photothermal instability laser power threshold P_{thp}.

To further demonstrate the capability of assembling particles into desired patterns and fabricating defect-free heterogeneous composite structures using the novel A-TPP process, a small amount of composite mixture with 0.5 wt.% iron oxide and 10 wt.% thiol was dropped onto the Kapton tape and the piezoelectric plate was actuated. Figures 4(*e*)–4(*g*) show the microscopic images of the prepared sample before and after applying an acoustic field at various frequencies. Concentric curve patterns with an approximate thickness of 35 μm were successfully formed using the novel acoustic field setup with 2.2 MHz frequency and 5 V peak-to-peak voltage, as shown in Fig. 4(*g*). A multi-material composite model was then printed using the patterned nanoparticle–polymer composite by the TPP process.

Figures 4(*h*) and 4(*i*) show the computer-aided design (CAD) model and an optical image of the letters "UIC" structures as an example. The letters were fabricated at a scanning speed and a laser power of 20 mm/s and 19%, respectively. The width of the structure was 25 μm, and the total size of each letter was about 150 μm. From the image of the fabricated part shown in Fig. 4(*i*), the locally distributed iron oxide nanoparticles along the center can be observed. It shows the capability of the proposed A-TPP process for fabricating nanoparticle–polymer composites with controlled particle distribution patterns. This result also validated our hypothesis that the two-photon curing of nanoparticle–polymer composite with acoustically assembled nanoparticle patterns is possible by balancing threshold laser powers.

4 Conclusion

This work addressed the crucial photothermal effect challenge in patterning and curing nanoparticles in the liquid resin during acoustic assembling and two-photon polymerization. A novel acoustic field-assisted Two-Photon Polymerization (A-TPP) method is developed to fabricate patterned nanoparticle–polymer composite microstructures, by integrating acoustic field into the two-photon polymerization process and identifying appropriate process parameter settings. Desired particle patterns and their local distributions were planned and controlled using an external acoustic field. An empirical model was developed for identifying the minimum thiol concentration and safe laser power to cure the resin composite with desired particle patterns. Test cases were fabricated to validate the feasibility of the proposed A-TPP process on the production of nanoparticle–polymer composite microstructures with locally controlled particle distributions by balancing threshold laser powers for polymerization and photothermal instability.

Future work will focus on integrating the effect of process settings including writing speed and hatching distance, on the NP assembly printing results, to achieve printing anisotropic composites or multi-material microstructures with a high material accuracy and geometry accuracy.

Acknowledgment

This material is based upon work partially supported by the National Science Foundation (Grant Number No. 1663399). The authors are thankful to the NSF support and the Electron Microscopy Service from the UIC Nanotechnology Core Facility.

Conflict of Interest

There are no conflicts of interest.

Data Availability Statement

The data sets generated and supporting the findings of this article are obtainable from the corresponding author upon reasonable request. The authors attest that all data for this study are included in the paper. Data provided by a third party are listed in Acknowledgment.

References

[1] Trotta, G., Stampone, B., Fassi, I., and Tricarico, L., 2021, "Study of Rheological Behaviour of Polymer Melt in Micro Injection Moulding With a Miniaturized Parallel Plate Rheometer," Polym. Test., **96**, p. 107068.

[2] Azizipour, N., Avazpour, R., Rosenzweig, D. H., Sawan, M., and Ajji, A., 2020, "Evolution of Biochip Technology: A Review From Lab-on-a-Chip to Organ-on-a-Chip," Micromachines, **11**(6), p. 599.

[3] Wang, X., Yu, H., Li, P., Zhang, Y., Wen, Y., Qiu, Y., Liu, Z., Li, Y., and Liu, L., 2021, "Femtosecond Laser-Based Processing Methods and Their Applications in Optical Device Manufacturing: A Review," Opt. Laser Technol., **135**, p. 106687.

[4] Lee, K. S., Kim, R. H., Yang, D. Y., and Park, S. H., 2008, "Advances in 3D Nano/Microfabrication Using Two-Photon Initiated Polymerization," Prog. Polym. Sci., **33**(6), pp. 631–681.

[5] Xia, Y., Rogers, J. A., Paul, K. E., and Whitesides, G. M., 1999, "Unconventional Methods for Fabricating and Patterning Nanostructures," Chem. Rev., **99**(7), pp. 1823–1848.

[6] Madden, J. D., and Hunter, I. W., 1996, "Three-Dimensional Microfabrication by Localized Electrochemical Deposition," J. Microelectromech. Syst., **5**(1), pp. 24–32.

[7] Malinauskas, A., 2001, "Chemical Deposition of Conducting Polymers," Polymer, **42**(9), pp. 3957–3972.

[8] Ikariyama, Y., Yamauchi, S., Yukiashi, T., and Ushioda, H., 1987, "Micro-enzyme Electrode Prepared on Platinized Platinum," Anal. Lett., **20**(9), pp. 1407–1416.

[9] Chen, F., Zhang, D., Yang, Q., Yong, J., Du, G., Si, J., Yun, F., and Hou, X., 2013, "Bioinspired Wetting Surface via Laser Microfabrication," ACS Appl. Mater. Interfaces, **5**(15), pp. 6777–6792.

[10] Hatakeyama, M., Ichiki, K., Satake, T., Hatamura, Y., Nakao, M., and Ebara Corp, 2003, "Microfabrication of pattern imprinting," U.S. Patent 6,671,034.

[11] Pao, Y. H., and Rentzepis, P. M., 1965, "Laser-Induced Production of Free Radicals in Organic Compounds," Appl. Phys. Lett., **6**(5), pp. 93–95.

[12] Lei, S., Zhao, X., Yu, X., Hu, A., Vukelic, S., Jun, M. B. G., Joe, H., Yao, Y. L., and Shin, Y. C., 2020, "Ultrafast Laser Applications in Manufacturing Processes: A State-of-the-Art Review," ASME. J. Manuf. Sci. Eng., **142**(3), p. 031005.

[13] Ushiba, S., Shoji, S., Masui, K., Kuray, P., Kono, J., and Kawata, S., 2013, "3D Microfabrication of Single-Wall Carbon Nanotube/Polymer Composites by Two-Photon Polymerization Lithography," Carbon, **59**, pp. 283–288.

[14] Lichade, K., Jiang, Y., and Pan, Y., 2021, "Hierarchical Nano/Micro-structured Surfaces With High Surface Area/Volume Ratios," ASME J. Manuf. Sci. Eng., **143**(8), pp. 1–36.

[15] Ledermann, A., Cademartiri, L., Hermatschweiler, M., Toninelli, C., Ozin, G. A., Wiersma, D. S., Wegener, M., and Von Freymann, G., 2006, "Three-Dimensional Silicon Inverse Photonic Quasicrystals for Infrared Wavelengths," Nat. Mater., **5**(12), pp. 942–945.

[16] Rill, M. S., Plet, C., Thiel, M., Staude, I., Von Freymann, G., Linden, S., and Wegener, M., 2008, "Photonic Metamaterials by Direct Laser Writing and Silver Chemical Vapour Deposition," Nat. Mater., **7**(7), pp. 543–546.

[17] Maruo, S., Ikuta, K., and Korogi, H., 2003, "Submicron Manipulation Tools Driven by Light in a Liquid," Appl. Phys. Lett., **82**(1), pp. 133–135.

[18] Tayalia, P., Mendonca, C. R., Baldacchini, T., Mooney, D. J., and Mazur, E., 2008, "3D Cell-Migration Studies Using Two-Photon Engineered Polymer Scaffolds," Adv. Mater., **20**(23), pp. 4494–4498.

[19] Song, J., Michas, C., Chen, C. S., White, A. E., and Grinstaff, M. W., 2020, "From Simple to Architecturally Complex Hydrogel Scaffolds for Cell and Tissue Engineering Applications: Opportunities Presented by Two-Photon Polymerization," Adv. Healthcare Mater., **9**(1), p. 1901217.

[20] Cumpston, B. H., Ananthavel, S. P., Barlow, S., Dyer, D. L., Ehrlich, J. E., Erskine, L. L., Heikal, A. A., Kuebler, S. M., Lee, I. Y. S., McCord-Maughon, D., and Qin, J., 1999, "Two-Photon Polymerization Initiators for Three-Dimensional Optical Data Storage and Microfabrication," Nature, **398**(6722), pp. 51–54.

[21] Gissibl, T., Wagner, S., Sykora, J., Schmid, M., and Giessen, H., 2017, "Refractive Index Measurements of Photo-Resists for Three-Dimensional Direct Laser Writing," Opt. Mater. Express, **7**(7), pp. 2293–2298.

[22] Ostendorf, A., and Chichkov, B. N., 2006, "Two-Photon Polymerization: a New Approach to Micromachining," Photonics spectra, **40**(10), p. 72.

[23] Chueh, Y., Zhang, X., Wei, C., Sun, Z., and Li, L., 2020, "Additive Manufacturing of Polymer-Metal/Ceramic Functionally Graded Composite Components via Multiple Material Laser Powder Bed Fusion," ASME J. Manuf. Sci. Eng., **142**(5), p. 051003.

[24] Le, B., Khaliq, J., Huo, D., Teng, X., and Shyha, I., 2020, "A Review on Nanocomposites. Part 1: Mechanical Properties," ASME J. Manuf. Sci. Eng., **142**(10), p. 100801.

[25] Gong, S., Cui, W., Zhang, Q., Cao, A., Jiang, L., and Cheng, Q., 2015, "Integrated Ternary Bioinspired Nanocomposites via Synergistic Toughening of Reduced Graphene Oxide and Double-Walled Carbon Nanotubes," ACS Nano, **9**(12), pp. 11568–11573.

[26] Ishitobi, H., Shoji, S., Hiramatsu, T., Sun, H. B., Sekkat, Z., and Kawata, S., 2008, "Two-Photon Induced Polymer Nanomovement," Optics Express, **16**(18), pp. 14106–14114.

[27] Sun, Z. B., Dong, X. Z., Chen, W. Q., Nakanishi, S., Duan, X. M., and Kawata, S., 2008, "Multicolor Polymer Nanocomposites: In situ Synthesis and Fabrication of 3D Microstructures," Adv. Mater., **20**(5), pp. 914–919.

[28] Kaneko, K., Sun, H. B., Duan, X. M., and Kawata, S., 2003, "Two-Photon Photoreduction of Metallic Nanoparticle Gratings in a Polymer Matrix," Appl. Phys. Lett., **83**(7), pp. 1426–1428.

[29] Xia, H., Wang, J., Tian, Y., Chen, Q. D., Du, X. B., Zhang, Y. L., He, Y., and Sun, H. B., 2010, "Ferrofluids for Fabrication of Remotely Controllable Micro-nano-machines by Two-Photon Polymerization," Adv. Mater., **22**(29), pp. 3204–3207.

[30] Liu, Y., Xiong, W., Jiang, L. J., Zhou, Y. S., and Lu, Y. F., 2016, "Precise 3D Printing of Micro/Nanostructures Using Highly Conductive Carbon Nanotube-Thiol-Acrylate Composites," Laser 3D Manufacturing III, San Francisco, CA, Apr. 6.

[31] Ovsianikov, A., Viertl, J., Chichkov, B., Oubaha, M., MacCraith, B., Sakellari, I., Giakoumaki, A., Gray, D., Vamvakaki, M., Farsari, M., and Fotakis, C., 2008, "Ultra-low Shrinkage Hybrid Photosensitive Material for Two-Photon Polymerization Microfabrication," ACS Nano, **2**(11), pp. 2257–2262.

[32] Roy, M., Tran, P., Dickens, T., and Schrand, A., 2020, "Composite Reinforcement Architectures: A Review of Field-Assisted Additive Manufacturing for Polymers," J. Compos. Sci., **4**(1), p. 1.

[33] Joyee, E. B., Lu, L., and Pan, Y., 2019, "Analysis of Mechanical Behavior of 3D Printed Heterogeneous Particle-Polymer Composites," Composites, Part B, **173**, p. 106840.

[34] Niendorf, K., and Raeymaekers, B., 2021, "Additive Manufacturing of Polymer Matrix Composite Materials With Aligned or Organized Filler Material: A Review," Adv. Eng. Mater., p. 2001002.

[35] Vekselman, V., Sande, L., and Kornev, K. G., 2015, "Fully Magnetic Printing by Generation of Magnetic Droplets on Demand With a Coilgun," J. Appl. Phys., **118**(22), p. 224902.

[36] Martin, J. J., Fiore, B. E., and Erb, R. M., 2015, "Designing Bioinspired Composite Reinforcement Architectures via 3D Magnetic Printing," Nat. Commun., **6**(1), pp. 1–7.

[37] Lu, L., Guo, P., and Pan, Y., 2017, "Magnetic-Field-Assisted Projection Stereolithography for Three-Dimensional Printing of Smart Structures," ASME J. Manuf. Sci. Eng., **139**(7), p. 071008.

[38] Kim, Y., Yuk, H., Zhao, R., Chester, S. A., and Zhao, X., 2018, "Printing Ferromagnetic Domains for Untethered Fast-Transforming Soft Materials," Nature, **558**(7709), pp. 274–279.

[39] Holmes, L. R., and Riddick, J. C., 2014, "Research Summary of an Additive Manufacturing Technology for the Fabrication of 3D Composites With Tailored Internal Structure," Jom, **66**(2), pp. 270–274.

[40] Yang, Y., Chen, Z., Song, X., Zhang, Z., Zhang, J., Shung, K. K., Zhou, Q., and Chen, Y., 2017, "Biomimetic Anisotropic Reinforcement Architectures by Electrically Assisted Nanocomposite 3D Printing," Adv. Mater., **29**(11), p. 1605750.

[41] Lee, C., and Tarbutton, J. A., 2014, "Electric Poling-Assisted Additive Manufacturing Process for PVDF Polymer-Based Piezoelectric Device Applications," Smart Mater. Struct., **23**(9), p. 095044.

[42] Kim, G. H., Shkel, Y. M., and Rowlands, R. E., 2003, "Field-Aided Microtailoring of Polymeric Nanocomposites," Smart Structures and Materials 2003: Electroactive Polymer Actuators and Devices, San Diego, CA, July 28.

[43] Yunus, D. E., Sohrabi, S., He, R., Shi, W., and Liu, Y., 2017, "Acoustic Patterning for 3D Embedded Electrically Conductive Wire in Stereolithography," J. Micromech. Microeng., **27**(4), p. 045016.

[44] Collino, R. R., Ray, T. R., Fleming, R. C., Cornell, J. D., Compton, B. G., and Begley, M. R., 2016, "Deposition of Ordered Two-Phase Materials Using Microfluidic Print Nozzles With Acoustic Focusing," Extreme Mech. Lett., **8**, pp. 96–106.

[45] Hahnlen, R., and Dapino, M. J., 2014, "NiTi–Al Interface Strength in Ultrasonic Additive Manufacturing Composites," Composites, Part B, **59**, pp. 101–108.

[46] Lu, L., Tang, X., Hu, S., and Pan, Y., 2018, "Acoustic Field-Assisted Particle Patterning for Smart Polymer Composite Fabrication in Stereolithography," 3D Print. Addit. Manuf., **5**(2), pp. 151–159.

[47] Asif, S., Chansoria, P., and Shirwaiker, R., 2020, "Ultrasound-Assisted vat Photopolymerization 3D Printing of Preferentially Organized Carbon Fiber Reinforced Polymer Composites," J. Manuf. Process., **56**, pp. 1340–1343.

[48] Coakley, W. T., Bardsley, D. W., Grundy, M. A., Zamani, F., and Clarke, D. J., 1989, "Cell Manipulation in Ultrasonic Standing Wave Fields," J. Chem. Technol. Biotechnol., **44**(1), pp. 43–62.

[49] Petersson, F., Åberg, L., Swärd-Nilsson, A. M., and Laurell, T., 2007, "Free Flow Acoustophoresis: Microfluidic-Based Mode of Particle and Cell Separation," Anal. Chem., **79**(14), pp. 5117–5123.

[50] Yang, Y., Song, X., Li, X., Chen, Z., Zhou, C., Zhou, Q., and Chen, Y., 2018, "Recent Progress in Biomimetic Additive Manufacturing Technology: From Materials to Functional Structures," Adv. Mater., **30**(36), p. 1706539.

[51] Masui, K., Shoji, S., Asaba, K., Rodgers, T. C., Jin, F., Duan, X. M., and Kawata, S., 2011, "Laser Fabrication of Au Nanorod Aggregates Microstructures Assisted by Two-Photon Polymerization," Optics Express, **19**(23), pp. 22786–22796.

[52] Blasco, E., Müller, J., Müller, P., Trouillet, V., Schön, M., Scherer, T., Barner-Kowollik, C., and Wegener, M., 2016, "Fabrication of Conductive 3D Gold-Containing Microstructures via Direct Laser Writing," Adv. Mater., **28**(18), pp. 3592–3595.

[53] Liu, Y., Hu, Q., Zhang, F., Tuck, C., Irvine, D., Hague, R., He, Y., Simonelli, M., Rance, G. A., Smith, E. F., and Wildman, R. D., 2016, "Additive Manufacture of Three Dimensional Nanocomposite Based Objects Through Multiphoton Fabrication," Polymers, **8**(9), p. 325.

[54] Hu, Q., Sun, X. Z., Parmenter, C. D., Fay, M. W., Smith, E. F., Rance, G. A., He, Y., Zhang, F., Liu, Y., Irvine, D., and Tuck, C., 2017, "Additive Manufacture of Complex 3D Au-Containing Nanocomposites by Simultaneous Two-Photon Polymerisation and Photoreduction," Sci. Rep., **7**(1), pp. 1–9.

[55] Jiang, L., Xiong, W., Zhou, Y., Liu, Y., Huang, X., Li, D., Baldacchini, T., Jiang, L., and Lu, Y., 2016, "Performance Comparison of Acrylic and Thiol-Acrylic Resins in Two-Photon Polymerization," Optics Express, **24**(12), pp. 13687–13701.

[56] Wolfberger, A., Rupp, B., Kern, W., Griesser, T., and Slugovc, C., 2011, "Ring Opening Metathesis Polymerization Derived Polymers as Photoresists: Making Use of Thiol-ene Chemistry," Macromol. Rapid Commun., **32**(6), pp. 518–522.
[57] Quick, A. S., Fischer, J., Richter, B., Pauloehrl, T., Trouillet, V., Wegener, M., and Barner-Kowollik, C., 2013, "Preparation of Reactive Three-Dimensional Microstructures via Direct Laser Writing and Thiol-ene Chemistry," Macromol. Rapid Commun., **34**(4), pp. 335–340.
[58] Lafleur, L. K., Dong, J., and Parviz, B. A., 2005, "Using Molecular Monolayers as Self-Assembled Photoresist," The 13th International Conference on Solid-State Sensors, Actuators and Microsystems, 2005. Digest of Technical Papers. TRANSDUCERS'05, Seoul, South Korea, June 5–9.
[59] Wadsworth, P., Nelson, I., Porter, D. L., Raeymaekers, B., and Naleway, S. E., 2020, "Manufacturing Bioinspired Flexible Materials Using Ultrasound Directed Self-assembly and 3D Printing," Mater. Des., **185**, p. 108243.
[60] Samarasekera, C., and Yeow, J. T., 2015, "Facile Microfluidic Channels for Acoustophoresis on a Budget," Biomed. Microdevices, **17**(5), pp. 1–8.
[61] Soto, F., Wagner, G. L., Garcia-Gradilla, V., Gillespie, K. T., Lakshmipathy, D. R., Karshalev, E., Angell, C., Chen, Y., and Wang, J., 2016, "Acoustically Propelled Nanoshells," Nanoscale, **8**(41), pp. 17788–17793.